Received: 23 December 2025 | Revised: 30 March 2026 | Accepted: 20 April 2026| Published online: 7 May 2026

RESEARCH ARTICLE

Medinformatics
2026, Vol. 00(00) 1–15
DOI: 10.47852/bonviewMEDIN62028877

BON VIEW PUBLISHING

Phytochemicals from *Amaranthus tricolor* L. with Potential Anti-Inflammatory Activity: An *In Silico* Molecular Docking, QSAR, and ADMET Study

Ferdousi Ahmed Sumona[1, †], Sawda Binta Kamrul Oishi[1, †], Md. Rakibul Hossain[1], Sumaiya Khatun[1] and Ayesha Islam Sadia[2], Md. Sabbir Hossain[3], Md. Abu Bakar Siddique Jami[2, 4, *]

[1] *Department of Pharmacy, Bangladesh University, Bangladesh*

[2] *Department of Pharmacy, East West University, Bangladesh*

[3] *Department of Pharmacy, Pabna University of Science and Technology, Bangladesh*

[4] *Department of Pharmacy, University of Information Technology and Sciences, Bangladesh*

Abstract: Inflammation is a complex biological response that contributes to the pathogenesis of many chronic diseases. Cyclooxygenase-2 (COX-2) plays a central role in inflammatory processes by catalyzing the synthesis of proinflammatory prostaglandins. Natural COX-2 inhibitors have gained increasing interest as potential alternatives to synthetic drugs due to their improved safety profiles. *Amaranthus tricolor* L., a leafy vegetable, is traditionally recognized for its anti-inflammatory and antioxidant properties. This study investigated the anti-inflammatory potential of major phytochemicals from *A. tricolor* using an integrated *in silico* approach involving molecular docking, ADMET profiling, and quantitative structure–activity relationship (QSAR) analysis to identify promising COX-2 inhibitors. A total of thirty-three phytocompounds reported in *A. tricolor* were identified and screened against the crystal structure of COX-2 enzyme (PDB: 1CX2) using molecular docking. Diclofenac was employed as a reference drug. Docking was performed using PyRx, binding interactions were visualized using BIOVIA Discovery Studio. The physicochemical, pharmacokinetic, drug-likeness properties of the top-scoring ligands were evaluated using SwissADME, admetSAR, ChemDes, and pkCSM. Docking results revealed that myricetin-3-O-rutinoside exhibited the strongest binding affinity (−10.2 kcal/mol), exceeding that of diclofenac (−7.0 kcal/mol), followed by myricetin (−9.9 kcal/mol), quercetin (−9.5 kcal/mol), and a few others. These compounds formed stable interactions with active-site residues of COX-2. ADMET and QSAR analyses indicated favorable absorption, moderate bioavailability, and acceptable safety profiles for most top ligands, while toxicity prediction suggested low hepatotoxicity and mutagenicity risks. The findings highlight myricetin, quercetin derivatives, and several other phytocompounds from *A. tricolor* as promising COX-2 inhibitors with potential anti-inflammatory activity.

Keywords: *Amaranthus tricolor*, COX-2, molecular docking, ADMET, QSAR

1. Introduction

Inflammation is a complex biological response of the immune system to infection, tissue injury, or cellular stress [1, 2]. Even though acute inflammation is crucial to host defense and tissue repair, chronic inflammation is considered pathological and is closely associated with the progression of numerous disorders, including arthritis, cardiovascular diseases, diabetes, neurodegenerative conditions, and certain cancers [3, 4]. Persistent inflammatory responses lead to excessive production of proinflammatory mediators such as cytokines, prostaglandins, and reactive oxygen species, which ultimately result in tissue damage and organ dysfunction [5]. Cyclooxygenase-2 (COX-2) plays a pivotal role in this process by catalyzing the synthesis of proinflammatory prostaglandins, making it a major therapeutic target in the management of inflammatory diseases [6, 7].

Currently used nonsteroidal anti-inflammatory drugs (NSAIDs) primarily exert their effects through inhibition of COX enzymes. However, long-term use of these agents is frequently associated with gastrointestinal, cardiovascular, and renal adverse effects [8]. These safety concerns have emphasized the need for alternative anti-inflammatory agents with improved

***Corresponding author:** Md. Abu Bakar Siddique Jami, Department of Pharmacy, East West University, and Department of Pharmacy, University of Information Technology and Sciences, Bangladesh. Email: abs.jami@uits.ac.bd

tolerability. Natural products were investigated and used more as a treatment of inflammatory conditions in recent times, due to their greater therapeutic properties and lower side effects than synthetic drugs have [9–11].

Medicinal plants contain a wide range of bioactive phytochemical classes that contribute to their therapeutic effects. Alkaloids, coumarins, flavonoids, phenolic compounds, glycosides, steroids, saponins, terpenoids, and tannins have been reported to show anti-inflammatory activity by diverse mechanisms, including inhibition of inflammatory enzymes, modulation of cytokine signaling, antioxidant activity, and immune regulation [12–14]. The coexistence of multiple phytochemicals within plant matrices often results in synergistic interactions, enhancing overall pharmacological efficacy and supporting their traditional medicinal use.

Amaranthus tricolor L. is a popular leafy vegetable and medicinal plant that has a rich history of use in traditional systems of medicine [15–17]. The species has a broad geographical range in Central Asia, South Asia (Sri Lanka, India, Bangladesh), East Asia (Japan, China, including Taiwan and Tibet, and Korea), Northeast Africa, Angola, Mozambique, Central America, the Caribbean, Australia, and part of Europe, including France [16, 18, 19]. The taxonomic hierarchy of this plant is shown in Table 1. Many *in vitro* and *in vivo* studies have demonstrated its antioxidant, antimicrobial, antidiabetic, hepatoprotective, anti-ulcer, and anti-inflammatory activities using crude extracts and solvent fractions of the plant [20–22]. Phytochemical investigations of *A. tricolor* leaves have consistently identified flavonoids, phenolic acids, tannins, glycosides, betalains, and related secondary metabolites as major constituents [16, 23]. While extract-based experimental studies have confirmed the pharmacological potential of *A. tricolor*, the specific contribution and molecular interactions of individual phytochemical compounds that are responsible for its anti-inflammatory properties remain insufficiently explored at the computational level.

Bangladesh has a lot of traditional medicinal plants used in the management of inflammatory disorders [24]. *A. tricolor* represents one such culturally and therapeutically significant species. In Bangladesh, the practice of self-medication using traditional and alternative plant-based remedies is highly prevalent [10, 25]. The present study focuses on the systematic *in silico* evaluation of phytochemicals reported in *A. tricolor* to elucidate their potential anti-inflammatory mechanisms. To the best of our knowledge, no comprehensive *in silico* anti-inflammatory study targeting the COX-2 enzyme has yet been conducted using the individual phytochemicals identified from *A. tricolor*. To address this research gap, molecular docking was performed against the COX-2 enzyme, followed by quantitative structure–activity relationship (QSAR) modeling, ADMET profiling, and toxicity prediction, to identify promising natural COX-2 inhibitors and to provide a rational basis for future compound-specific experimental validation.

2. Materials and Methods

Figure 1 shows the general workflow of the study. The study involved a sequential computational approach beginning with the identification of phytochemicals from *A. tricolor* L. A complete list of phytochemical constituents previously reported in *A. tricolor* was compiled primarily from the MPDB 2.0 (Medicinal Plant Database of Bangladesh, https://www.medicinalplantbd.com), an extensive repository containing phytochemical information for more than 500 Bangladeshi medicinal plants. We focused on the information and the primary phytochemical constituents of *A. tricolor*, as demonstrated in Table 2. Through this process, 33 phytocompounds were catalogued, along with their corresponding PubChem CIDs, to form the ligand database.

For the molecular docking study, the 3D chemical structures of all chosen phytochemicals were obtained in SDF format from the PubChem database (https://pubchem.ncbi.nlm.nih.gov/). Each ligand was optimized using Avogadro software by applying geometry minimization, appropriate protonation at physiological pH, and hydrogen addition [28]. After optimization, the structures were converted to PDBQT format using Open Babel to ensure compatibility with AutoDock Vina. The crystal structure of the enzyme cyclooxygenase-2 (COX-2) was obtained in the RCSB Protein Data Bank (PDB ID: 1CX2). All the heteroatoms, other co-crystallized ligands, and water molecules were removed during the protein production process using BIOVIA Discovery Studio Visualizer. Open Babel was used to export the structure to PDBQT format with polar hydrogens and Kollman charges added. [29]. Figure 2 shows the clean and optimized structure of the protein.

The PyRx tool's integrated AutoDock Vina was used to perform molecular docking. A grid box was centered at the catalytic site of COX-2 with coordinates $X = 28.6825$, $Y = 28.5866$, $Z = 9.2950$ and dimensions of 58.3851 Å × 76.9422 Å × 64.8137 Å to encompass the active binding pocket. Docking simulations were

Table 1. Taxonomic hierarchy of *Amaranthus tricolor* L

Rank	Classification	References
Kingdom	Plantae	
Subkingdom	Tracheobionta	
Super division	Spermatophyta	
Phylum	Magnoliophyta	
Class	Magnoliopsida	
Subclass	Caryophyllidae	[18, 26, 27]
Order	Caryophyllales	
Family	Amaranthaceae	
Subfamily	Amaranthoideae	
Genus	*Amaranthus*	
Species	*Amaranthus tricolor*	

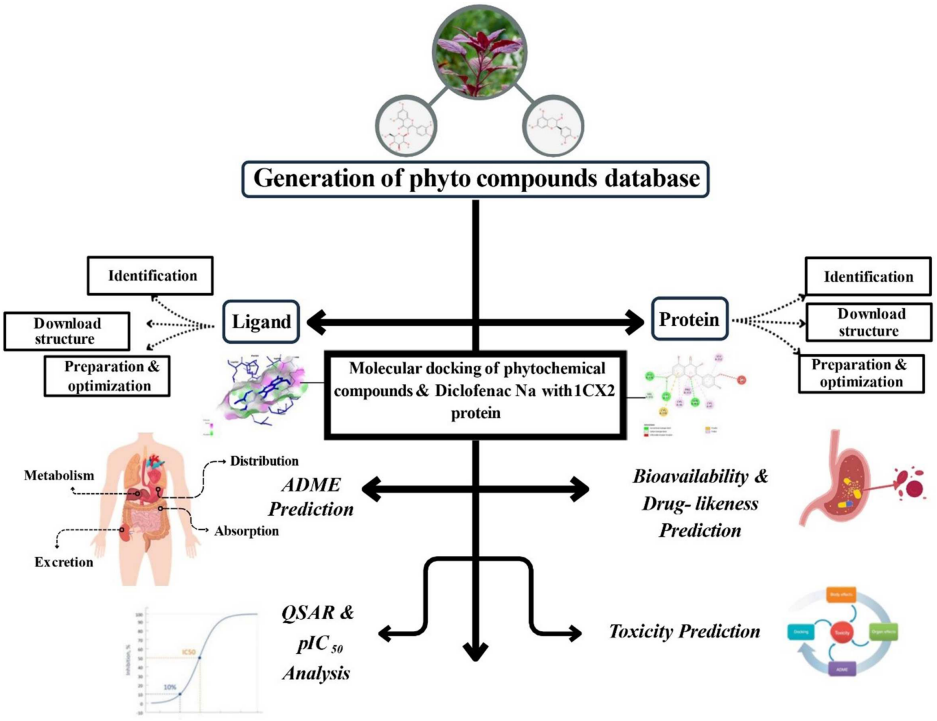

Figure 1. Methodology flow diagram

Table 2. Phytochemicals in *A. tricolor* L. that may serve as anti-inflammatory agents

Scientific name	Local name	Utilized part	Active compounds	Ref(s)
A. tricolor L.	Sanskrit: Marisarakta, Aramasitalika Bengali: Lal Shak English: Chinese Spinach, Garden Amaranth, Fountain Plant, Elephant Head Amaranth Ayurvedic: Maarisha-rakta (red variety) Siddha/Tamil: Arai-keerai, Siru-keerai, Thandu-keerai, Mulakkerai Folk: Laal Shaak, Laal Marashaa Gujarati: Tandaljo (Lal) Hindi: Lal Marsa Kannada: Dantu, Harave Soppu, Dantina Soppu, Chikkarive Malayalam: Aramaseetalam Marathi: Mash Punjabi: Lal Marsa Sag Tamil: Mulaikkeerai Telugu: Erra Tatakura	Leaf	4-Hydroxy-3,5-dimethoxy cinnamic acid, trans-cinnamic acid, 3-hydroxy cinnamic acid, 3,4-dihydroxy-trans-cinnamate, 4-hydroxy cinnamic acid, 3-methoxy-4-hydroxy cinnamic acid, quercetin-3-O-rutinoside, quercetin-3-O-galactoside, quercetin-3-O-glucoside, myricetin, quercetin, 5,7-dihydroxy-2-(4-hydroxyphenyl)-4-benzopyrone, kaempferol, catechin, 3-phenyl acrylic acid, 2-(3,4-dihydroxy phenyl)-3,5,7-trihydroxychromene-4-one, myricetin-3-O-rutinoside, kaempferol-3-O-rutinoside, tannic acid, amaranthin, betalain, β-xanthin, β-cyanin, 2-hydroxybenzoic acid, 4-hydroxy-3-methoxybenzoic acid, 3,4-dihydroxybenzoic acid, 3,4,5-trihydroxybenzoic acid, 2,5-dihydroxybenzoic acid, 2,4-dihydroxybenzoic acid, P-hydroxybenzoic acid, 3,5-dimethoxy-4-hydroxybenzoic acid, 2,3,7,8-tetrahydroxy-chromeno [5,4,3-cde] chromene-5,10-dione, 3-(3,4-dihydroxy cinnamoyl)quinic acid	[17, 19]

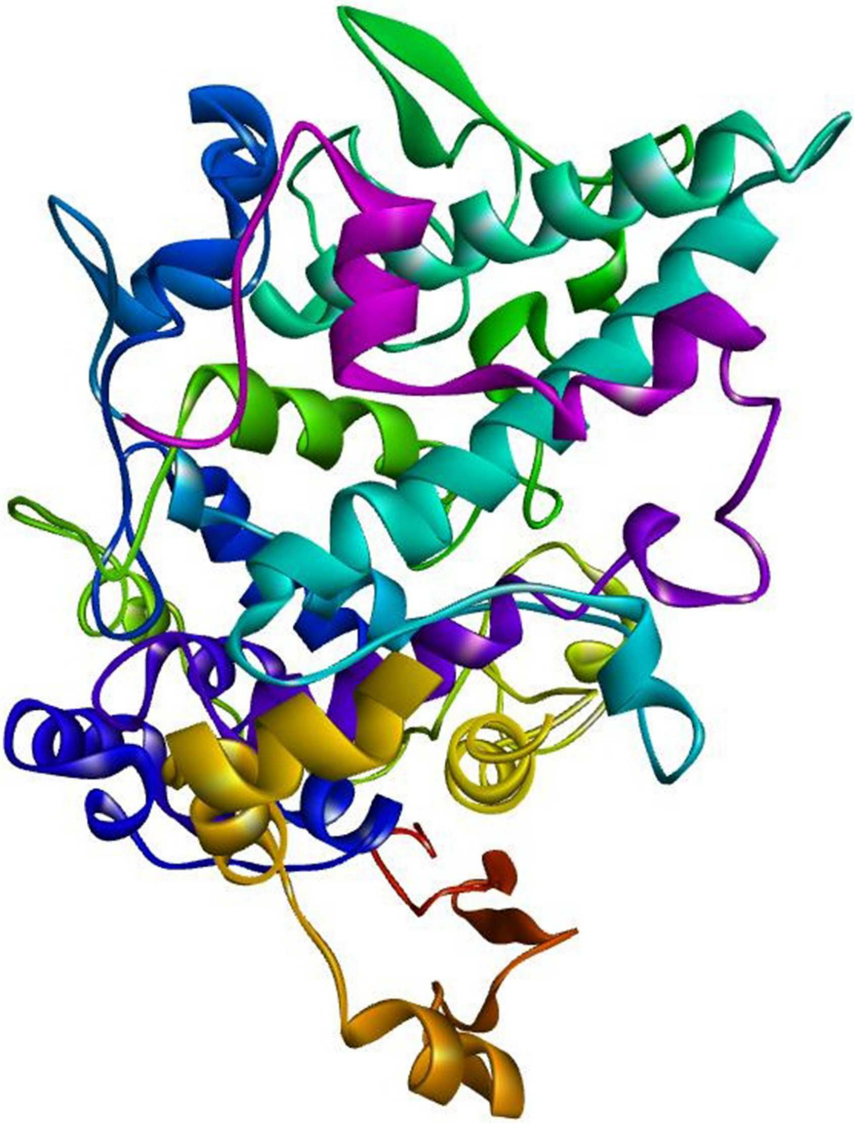

Figure 2. Optimized 3D crystal structure of the COX-2 (1CX2) protein

performed at default exhaustiveness parameters, and diclofenac was used as a reference COX-2 inhibitor for comparative evaluation. In order to examine binding positions, hydrogen-bond interactions, and residue contacts inside the active site, the resulting docked complexes were visualized in BIOVIA Discovery Studio [28].

Physicochemical profiling and pharmacokinetic predictions of the top-binding ligands were performed using several online platforms. SwissADME (https://swissadme.ch/index.php) and pkCSM (https://biosig.lab.uq.edu.au/pkcsm/prediction) were employed to examine solubility, lipophilicity, drug-likeness, bioavailability radar, and Lipinski's Rule of Five. Human intestinal absorption (HIA), blood–brain barrier (BBB) permeability, cytochrome P450 isoform metabolism, clearance parameters, and toxicity-related endpoints were among the other ADMET characteristics that were evaluated [30]. Canonical SMILES strings obtained from PubChem served as input for these computational evaluations to maintain structural consistency across prediction models [31].

Toxicity predictions were generated using the ProTox-3.0 (https://biosig.lab.uq.edu.au/pkcsm/predictionProTox-3.0) webserver [32], which applies similarity-based modeling and machine-learning classifiers to estimate hepatotoxicity, nephrotoxicity, carcinogenicity, cytotoxicity, and acute oral toxicity (LD_{50}). Each ligand was evaluated across 61 toxicity endpoints to generate a comprehensive toxicity profile and to compare safety differences between natural compounds and the reference drug diclofenac.

The inhibitory potency of the chosen drugs was predicted using QSAR analysis. The ChemDes web platform was utilized to compute molecular descriptors (http://www.scbdd.com/chemopy_desc/index/), from which several well-recognized descriptors, Chiv5, Bcutm1, MRVSA9, MRVSA6, PEOE VSA5, GATSv4, J index, and molecular diameter, were extracted. These descriptors were used to estimate pIC_{50} values, allowing an assessment of predicted biological activity that complements the docking results [33].

The ecological toxicity assessments were performed using admetSAR 3.0 (https://lmmd.ecust.edu.cn/admetsar3/predict.php) to evaluate Ames mutagenicity, avian toxicity, honey bee toxicity, crustacean and fish toxicity, *Tetrahymena pyriformis* toxicity, and biodegradability of the compounds [34]. The environmental safety of each phytochemical was compared with that

of diclofenac to determine whether the natural compounds pose a lower ecological risk.

3. Results

Molecular docking of the 33 phytochemicals identified from *A. tricolor* L. against the COX-2 enzyme (PDB: 1CX2) revealed that eight compounds, L8, L18, L21, L24, L25, L26, L29, and L32, exhibited the strongest binding affinities (with most negative values) and were therefore selected as the top candidates for further in-depth analysis (Table 3). Only compounds with docking scores better than the reference were advanced for further ADMET and QSAR analysis. The chemical structures of these eight ligands extracted from PubChem are shown in Figure 3. These ligands demonstrated docking scores ranging from −9.1 to −10.2 kcal/mol, all outperforming the reference drug diclofenac (−7.0 kcal/mol). The strongest binding was observed for myricetin-3-O-rutinoside (L29: −10.2 kcal/mol), followed by myricetin (L24: −9.9 kcal/mol), quercetin (L18: −9.5 kcal/mol), and compound L32 (–9.5 kcal/mol). Catechin (L8: −9.1 kcal/mol) and quercetin-3-O-rutinoside (L21: −9.0 kcal/mol) also exhibited substantially better affinity than the reference drug. The 2D and 3D interaction diagrams presented in Figure 4 illustrate that all eight ligands formed multiple stabilizing interactions, including hydrogen bonds, π–π stacking, and hydrophobic contacts, with key COX-2 active site residues.

Table 3. Binding affinity scores of *A. tricolor* L. identified molecules docked into the active sites of the COX-2 enzyme

Ligand No.	Compound name	PubChem CID	COX-2Binding affinity (kcal/mol)
Ref. Drug	Diclofenac	3033	–7.0
L1	3,4-Dihydroxybenzoic acid	72	–6.1
L2	P-hydroxybenzoic acid	135	–6.7
L3	2-Hydroxybenzoic acid	338	–6.5
L4	3,4,5-Trihydroxybenzoic acid	370	–6.2
L5	2,4-dihydroxybenzoic acid	1491	–6.6
L6	2,5-Dihydroxybenzoic acid	3469	–6.8
L7	4-Hydroxy-3-methoxybenzoic acid	8468	–5.9
L8	Catechin	9064	–9.1
L9	3,5-Dimethoxy-4-hydroxybenzoic acid	10742	–6.4
L10	Trans-cinnamic acid	444539	–6.4
L11	3-Methoxy-4-hydroxy cinnamic acid	445858	–6.6
L12	3-Hydroxy cinnamic acid	637541	–6.0
L13	4-Hydroxy cinnamic acid	637542	–6.9
L14	4-Hydroxy-3,5-dimethoxy cinnamic acid	637775	–6.9
L15	3,4-Dihydroxy-trans-cinnamate	689043	–6.9
L16	3-(3,4-Dihydroxy cinnamoyl)quinic acid	1794427	–7.7
L17	3-Phenyl acrylic acid	5273469	–7.1
L18	Quercetin	5280343	–9.5
L19	5,7-Dihydroxy-2-(4-hydroxyphenyl)-4-benzopyrone	5280443	–8.8
L20	Quercetin-3-O-glucoside	5280804	–8.5
L21	Quercetin-3-O-rutinoside	5280805	–9.0
L22	Kaempferol	5280863	–9.0
L23	Quercetin-3-O-galactoside	5281643	–8.3
L24	Myricetin	5281672	–9.9
L25	2,3,7,8-Tetrahydroxy-chromeno [5,4,3-cde] chromene-5,10-dione	5281855	–9.5
L26	Kaempferol-3-O-rutinoside	5318767	–9.4
L27	Amaranthin	6325284	–8.8
L28	Tannic acid	16129778	–8.4
L29	Myricetin-3-O-rutinoside	21577860	–10.2
L30	Betalain	56841626	–8.2
L31	β-cyanin	112500418	–8.7
L32	2-(3,4-Dihydroxy phenyl)-3,5,7-trihydroxychromene-4-one	130367129	–9.5
L33	β-xanthin	135926572	–8.7

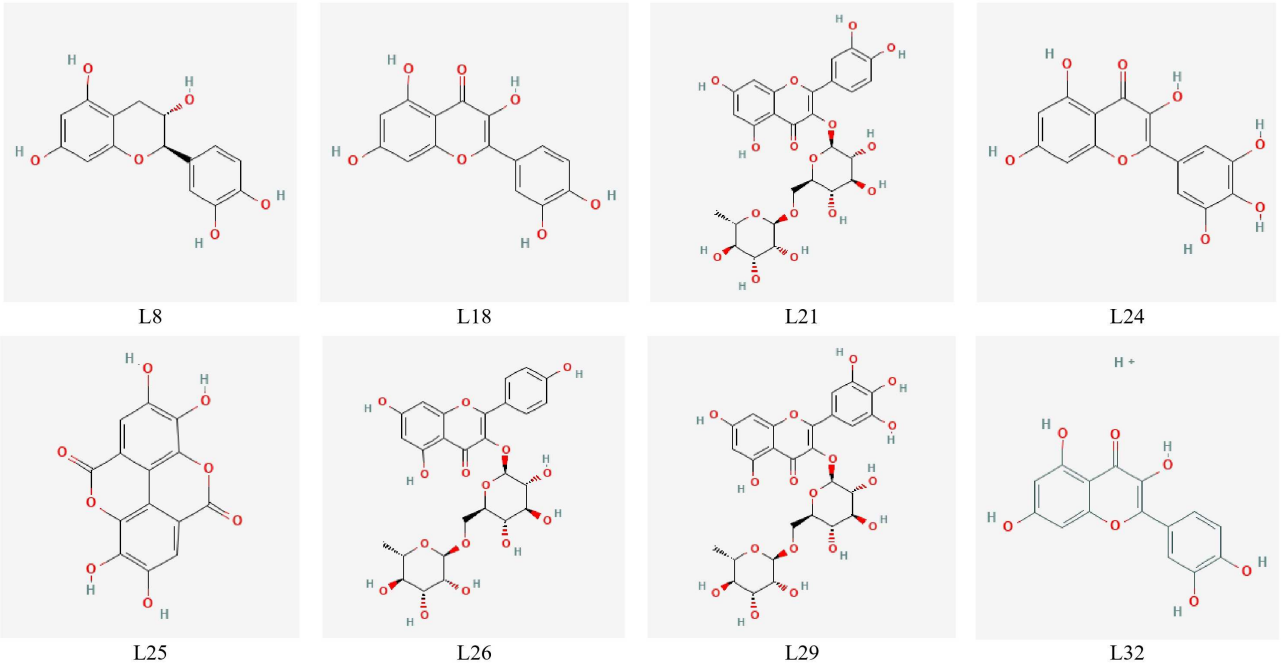

Figure 3. Chemical structures of the selected eight molecules from PubChem

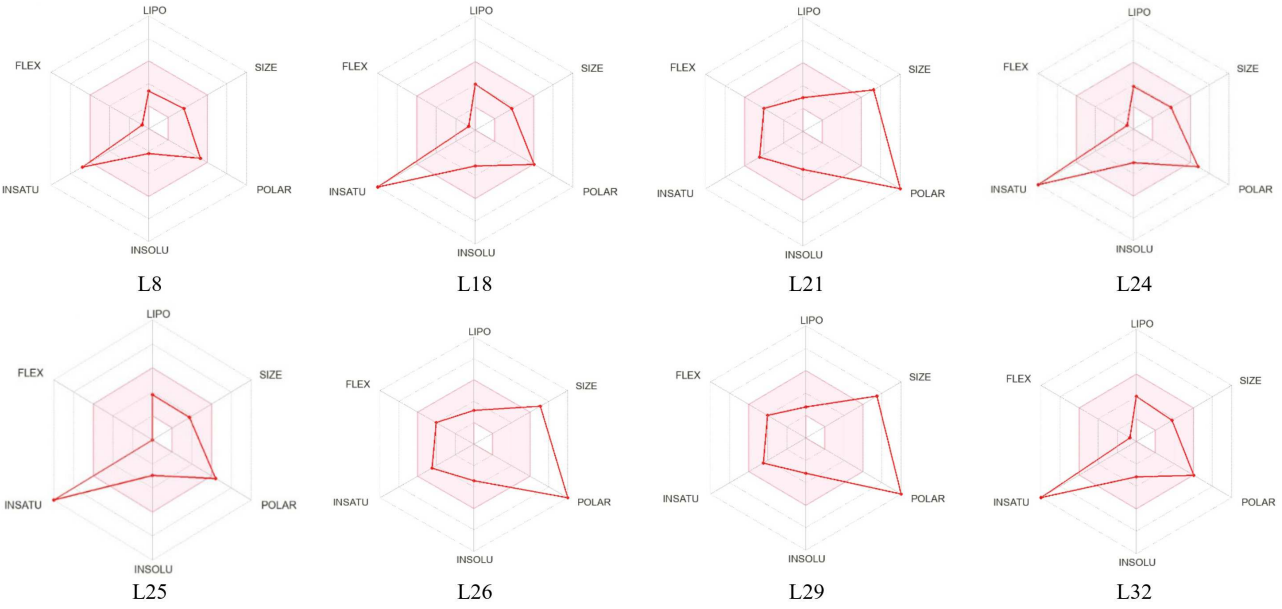

Figure 4. Bioavailability radars of the selected eight molecules

Evaluation of molecular properties (Table 4) revealed significant differences across the eight top molecules. Their molecular weights ranged widely from 290.27 g/mol (L8) to 626.52 g/mol (L29), with L21, L26, and L29 exceeding the ideal range for oral drug candidates due to glycosylation-related structural bulk. Hydrogen bonding capacity varied considerably, with the number of hydrogen bond acceptors ranging from 6 (L8) to 16 (L21) and donors from 4 (L25) to 11 (L29). Fraction Csp^3 values were low to moderate (0.00–0.44), indicating relatively planar structures, especially among flavonoids and polyphenols, whereas L26 and L29 exhibited slightly higher saturation due to sugar moieties. Topological polar surface area (TPSA) values ranged from 110.38 $Å^2$ (L8) to 289.66 $Å^2$ (L29), reflecting major differences in polarity and membrane permeability. Notably, L21, L26, and L29 showed TPSA well above the 140 $Å^2$ threshold, indicating poor predicted permeability despite excellent docking scores. Lipophilicity (Log P) also varied from −1.72 (L29) to 1.25 (L32), while solubility (Log S) ranged from −2.22 (L8) to −3.42 (L26). According to Lipinski's criteria, all compounds except L26 and L29 met acceptable drug-likeness requirements, although L21, L24, and L25 exhibited

Table 4. Molecular properties of the selected eight molecules and the reference drug

Parameter	L8	L18	L21	L24	L25	L26	L29	L32	Diclofenac
Molecular weight (g/mol)	290.27	302.24	610.52	318.24	302.19	594.52	626.52	303.24	296.15
H-bond acceptors	6	7	16	8	8	15	7	7	2
H-bond donors	5	5	10	6	4	9	11	5	2
Fraction Csp^3	0.20	0.00	0.00	0.00	0.00	0.44	0.44	0.00	0.07
TPSA ($Å^2$)	110.38	131.36	269.43	151.59	141.34	249.20	289.66	131.36	49.33
Log Po/w	0.83	1.23	–1.51	0.79	1.00	–1.13	–1.72	1.25	3.66
Log S (ESOL)	–2.22	–3.16	–3.30	–3.01	–2.94	–3.42	–3.16	–3.16	–4.65
Lipinski's rule	Yes, 0 violation	Yes, 0 violation	Yes, 1 violation	Yes, 1 violation	Yes, 0 violation	No, 3 violations	No, 3 violations	Yes, 0 violation	Yes, 0 violation
Bioavailability score	0.55	0.55	0.17	0.55	0.55	0.17	0.17	0.55	0.85

minor violations. These trends are also reflected in the bioavailability radar plots (Figure 4), which indicate that compounds L18 and L32 had an almost perfect physicochemical balance in all the parameters considered. The remaining molecules (L8, L21, L24, L25, L26, and L29) also demonstrated favorable characteristics, with only minor deviations.

ADMET profiling (Table 5) demonstrated diverse pharmacokinetic behaviors across the top molecules. HIA values varied significantly, with low absorption predicted for L21 (23.45%), L26 (30.74%), and L29 (14.07%), reflecting their high polarity and large TPSA values. In contrast, L25 (80.03%), L18 (77.21%), and L32 (77.39%) displayed considerably better absorption profiles. All molecules showed negative logBB values (< −1.05), indicating poor BBB penetration, which is desirable for peripherally acting anti-inflammatory agents. Central nervous system (CNS) permeability (logPS) showed similar trends, with highly negative values in L21 (−5.178), L29 (−5.397), and L26 (−5.015), suggesting minimal central nervous system exposure. None of the molecules acted as CYP3A4 inhibitors, and only L25 was classified as a substrate, indicating limited potential for cytochrome P450-mediated drug interactions. Total clearance rates ranged from −0.513 (L29) to 0.539 (L25), with diclofenac presenting a clearance value of 0.291. The MTD varied from 0.438 to 0.777 log mg/kg/day, suggesting moderate safety margins. Acute toxicity predictions (LD_{50}) ranged between 2.201 mol/kg (L25) and 2.513 mol/kg (L26), indicating moderate acute oral toxicity.

The predicted pIC_{50} values (Table 6) provided further understanding of the possible inhibitory effects of the chosen molecules. To determine the predicted pIC_{50} values, the following multiple linear regression equation was used:

$$\begin{aligned} pIC_{50} = {} & -2.768483965 + 0.133928895 \times Chi\_v5 \\ & + BCUTm1 - 0.02309681 \times MRVSA9 \\ & - 0.002946101 \times MRVSA6 + 0.00671218 \\ & \times PEOEVSA5 - 0.15963415 \times GATSv4 \\ & + 0.207949857 \times J + 0.082568569 \times Diametert \end{aligned}$$

These descriptors (Chiv5: Chi vertex connectivity index of order 5; BCUTm1: BCUT descriptor weighted by atomic mass; MRVSA9 and MRVSA6: molar refractivity VSA bins 9 and 6; PEOEVSA5: partial equalization of orbital electronegativities VSA bin 5; GATSv4: Geary autocorrelation of lag 4 weighted by van der Waals volume; J: Balaban J index; Diametert: topological molecular diameter) were computed for each ligand using ChemDes (http://www.scbdd.com/chemopy_desc/index/) [35]. The pIC_{50} values ranged from 4.38 (L25) to 5.43 (L29), indicating that most molecules fell within a pharmacologically relevant range. The highest pIC_{50} values were observed for L29 (5.43), L21 (5.41), and L26 (5.38), which align with their strong docking scores and extensive hydrogen-bonding interactions. Although catechin (L8) and quercetin (L18) exhibited relatively lower pIC_{50} values, both

Table 5. ADMET study of selected eight molecules and reference drug

Parameter	L8	L18	L21	L24	L25	L26	L29	L32	Diclofenac
Water solubility (log mol/L)	–3.117	2.925	–2.892	–2.915	–3.362	–2.900	–2.892	–2.925	–3.863
Human intestinal absorption (%)	68.829	77.207	23.446	65.930	80.032	30.743	14.071	77.395	91.923
BBB permeability (log BB)	–1.054	–1.098	–1.899	–1.493	–1.054	–1.669	–2.215	–1.116	0.236
CNS permeability (log PS)	–3.298	–3.065	–5.178	–3.709	–3.144	–5.015	–5.397	–3.050	–1.970
CYP3A4 substrate	No	No	No	No	Yes	No	No	No	No
CYP3A4 inhibitor	No	No	No	No	No	No	No	No	No
Total clearance (log ml/min/kg)	0.183	0.407	–0.369	0.422	0.539	–0.160	–0.513	0.246	0.291
Renal OCT2 substrate	No	No	No	No	No	No	No	No	No
Human Max. tolerated dose (log mg/kg/day)	0.438	0.499	0.452	0.510	0.777	0.481	0.441	0.499	0.983
Oral rat acute toxicity, LD50 (mol/kg)	2.428	2.471	2.491	2.497	2.201	2.513	2.484	2.472	2.405

Table 6. QSAR parameters and the pIC50 of the selected eight molecules and the reference drug

Ligand No.	Chiv5	Bcutm1	MRVSA9	MRVSA6	PEOEVSA5	GATSv4	J	Diametert	pIC_{50}
L8	1.751	3.950	0.0	41.459	6.066	1.011	1.670	10.0	4.72
L18	1.410	4.113	10.969	40.555	0	1.006	1.735	10.0	4.65
L21	3.269	4.122	10.969	40.555	0	1.017	1.322	17.0	5.41
L24	1.425	4.115	10.969	34.489	0	0.999	1.758	10.0	4.68
L25	1.933	4.272	32.711	32.973	0	1.219	1.746	9.0	4.38
L26	3.247	4.120	10.969	46.622	0	1.004	1.308	17.0	5.38
L29	3.285	4.123	10.969	34.489	0	1.017	1.337	17.0	5.43
L32	1.490	4.166	11.025	42.865	0	1.008	1.781	9	4.67
Diclofenac	1.344	4.039	40.546	58.073	47.467	0.956	1.936	9.0	4.08

remained within an acceptable potency range, reinforcing their relevance as potential COX-2 inhibitors.

Toxicity predictions derived from ProTox-3.0 (Table 7) indicated that all eight molecules were nonhepatotoxic, nonneurotoxic, and noncytotoxic. Nephrotoxicity was predicted across all ligands, while carcinogenicity was limited to four molecules (L18, L24, L25, and L32). Nutritional toxicity remained inactive for all ligands except L8, which showed active classification without clinical relevance. The LD_{50} values ranged from 159 mg/kg (L18, L24, L32) to 10,000 mg/kg (L8), placing them into toxicity classes III to VI. Diclofenac displayed a higher toxicity risk (class III). Notably, compounds L8 (class VI) and L25, L26, L29 (class V) were categorized as nontoxic or weakly toxic, while the reference drug diclofenac was more toxic (class III). These findings indicate that several of the selected phytochemicals possess comparatively lower toxicity risks than the standard reference drug.

Ecotoxicological assessment using admetSAR 3.0 (Table 8) indicated that all eight selected molecules exhibited low predicted toxicity toward microbial, avian, insect, crustacean, and aquatic species. Biodegradability scores were highest for L8 (0.486), L21 (0.306), and L29 (0.359), suggesting favorable environmental safety. Diclofenac, by contrast, showed significantly higher predicted toxicity toward crustaceans and fish and a much lower biodegradability score (0.106), reflecting the known environmental persistence of NSAIDs.

Table 7. The estimated toxicity properties of the selected eight molecules and the reference drug

Parameter	L8	L18	L21	L24	L25	L26	L29	L32	Diclofenac
Hepatotoxicity	Inactive	Inactive	Inactive	Inactive	Inactive	Inactive	Inactive	Inactive	Active
Neurotoxicity	Inactive	Inactive	Inactive	Inactive	Inactive	Inactive	Inactive	Inactive	Active
Nephrotoxicity	Active	Active	Active	Active	Active	Active	Active	Active	Active
Carcinogenicity	Inactive	Active	Inactive	Active	Active	Inactive	Inactive	Inactive	Inactive
Cytotoxicity	Inactive	Inactive	Inactive	Inactive	Inactive	Inactive	Inactive	Inactive	Inactive
Nutritional toxicity	Active	Active	Active	Active	Active	Active	Active	Active	Inactive
Predicted LD50 (mg/kg)	10000	159	5000	159	2991	5000	5000	159	53
Toxicity class	6	3	5	3	4	5	5	3	3

Table 8. Ecological risk and toxicity assessment

Ligand No.	Ames mutagenesis	Avian toxicity (*Colinus virginanus*)	Honey bee toxicity	Crustacean toxicity	Fish toxicity	*Tetrahymena pyriformis* toxicity	Biodegradability
L8	0.488	0.060	0.111	0.248	0.327	0.473	0.486
L18	0.616	0.102	0.095	0.467	0.536	0.970	0.172
L21	0.515	0.078	0.166	0.195	0.274	0.218	0.306
L24	0.527	0.101	0.102	0.435	0.501	0.813	0.161
L25	0.787	0.119	0.113	0.465	0.42	0.768	0.150
L26	0.588	0.098	0.185	0.216	0.314	0.268	0.212
L29	0.502	0.071	0.156	0.194	0.288	0.230	0.359
L32	0.631	0.104	0.090	0.471	0.552	0.952	0.158
Diclofenac	0.127	0.063	0.104	0.758	0.872	0.997	0.106

4. Discussion

Computational approaches such as molecular docking are frequently employed to predict the binding behavior of bioactive compounds toward therapeutic targets and to forecast their pharmacokinetic behavior in early-stage drug discovery [36]. In this study, docking analyses against the COX-2 enzyme (PDB: 1CX2) revealed that several phytochemicals from *A. tricolor* exhibit strong binding affinities, in some cases surpassing the reference drug diclofenac (−7.0 kcal/mol). The highest interaction strength was recorded for L29 (−10.2 kcal/mol), followed by L24 (−9.9 kcal/mol), L18, and L32 (−9.5 kcal/mol), while L8 and L21 also demonstrated notable affinities ranging from −9.1 to −9.0 kcal/mol. The presence of multiple polar, aromatic, and hydrophobic contacts within the active pocket of COX-2 suggests that these ligands may possess significant inhibitory potential. Hydrogen bonding patterns, in particular, play a critical role in determining the stability of protein–ligand complexes. Typically, strong hydrogen bonds fall within the range of 2.5–3.1 Å, whereas weaker bonds occur between 3.1 and 3.55 Å [37]. The interaction maps of the eight selected molecules (Figure 5) clearly illustrate the involvement of both polar and aromatic residues, and most ligands formed multiple stabilizing hydrogen bonds.

The binding affinities obtained in this study (−9.1 to −10.2 kcal/mol for the top eight ligands) suggest stronger predicted COX-2 binding compared with several previously published phytochemical docking studies. For instance, a docking study on *Gracilaria corticata* reported binding affinities ranging from −4.7 to −5.3 kcal/mol for major bioactive constituents, whereas the reference drug ibuprofen showed −6.5 kcal/mol [38]. In comparison, all top-ranked *A. tricolor* ligands in the present study exhibited substantially more favorable binding scores, exceeding the reference drug diclofenac (−7.0 kcal/mol). Similarly, in a previous *in silico* investigation of *Curcuma wallichii* phytoconstituents, reported COX-2 docking affinities ranged from −4.9 to −8.8 kcal/mol, with the strongest interaction observed for 2,9-dimethyl-3,4,5,10-tetrahydro-2H-azepinol[3,4-b]indol-1-one (−8.8 kcal/mol) [6]. Notably, the binding scores of myricetin-3-O-rutinoside (−10.2 kcal/mol), myricetin (−9.9 kcal/mol) and quercetin (−9.5 kcal/mol) in the present study were more negative than the top candidates reported in those studies, suggesting potentially stronger COX-2 binding. These features collectively reflect the strong theoretical affinity exhibited by the selected *A. tricolor* phytochemicals.

Assessment of molecular properties further contributes to understanding the drug-likeness and absorption potential of the tested molecules. The molecular weights of the selected compounds, ranging from 290.27 to 626.52 g/mol, fall within expected limits for plant-derived polyphenols and glycosides. While L21, L26, and L29 exceeded the ideal threshold for oral small molecules, the remaining ligands conformed to the generally accepted range for oral drug candidates [39]. Hydrogen bonding capacity, known to influence solubility and membrane permeability [40], varied considerably among the molecules. Compounds such as L21, L26, and L29 possessed a high number of hydrogen bond donors and acceptors, which, although contributing to enhanced docking interactions, may adversely affect passive membrane diffusion. Molecular flexibility, described by the fraction Csp^3, is a relevant parameter in early drug design because it influences solubility and conformational adaptability [41, 42]. L26 and L29 exhibited moderately higher saturation due to glycosylation, whereas the remaining molecules displayed low Csp^3 values, reflecting the rigid planar structure typical of flavonoids.

Membrane permeability largely depends on TPSA [43]. The TPSA values of most selected molecules remained below the recommended threshold of 140 $Å^2$, except for L21, L24, L25, L26, and L29, whose high polarity suggests poor predicted oral absorption. Lipophilicity, represented by Log P, further complemented these findings, indicating moderate lipophilicity across the dataset [44]. Solubility profiles (ESOL) revealed moderate to good solubility for the majority of compounds, with values superior to the reference drug, which may enhance dissolution rates [45]. In terms of bioavailability profiles, compounds L18 and L32 exhibited near-ideal physicochemical balance across all evaluated parameters. The remaining molecules (L8, L21, L24, L25, L26, and L29) also demonstrated favorable characteristics, with only minor deviations observed in one or two attributes, such as polarity or unsaturation.

The ADMET analysis revealed more information on the pharmacokinetic and safety profiles of the chosen molecules compared with diclofenac. HIA values varied from moderate to high across the majority of the molecules [46], though some compounds, such as L21, L26, and L29, exhibited lower absorption, consistent with their elevated polarity and TPSA values. Water solubility exhibited moderate variability, which may influence dissolution rates and formulation approaches. BBB permeability and CNS penetration (logPS) demonstrated consistently low values, indicating that the tested molecules are unlikely to cross into the central nervous system, which is advantageous for non-CNS therapeutic agents [30, 47]. None of the compounds inhibited CYP3A4, and only L25 was identified as a CYP3A4 substrate, suggesting minimal risk of CYP-mediated metabolic interactions [48]. Clearance values varied across the molecules, reflecting differences in predicted systemic elimination rates. The human maximum tolerated dose (MTD) values suggested that most compounds fall within acceptable dose-limiting toxicity thresholds [49]. Collectively, the ADMET results indicate that the selected candidates exhibit adequate oral absorption, limited CNS penetration, low CYP3A4 interaction potential, and moderate toxicity profiles, though solubility and high polarity may serve as limiting factors for certain molecules.

QSAR plays a central role in ligand-based drug design by elucidating relationships between structural and biological activities. The calculated QSAR descriptors and pIC_{50} values of the selected compounds supported the docking results and offered additional confidence in their theoretical inhibitory potential [50]. The pIC_{50} values, ranging from 4.38 to 5.43, indicate that most compounds possess meaningful predicted potency against the COX-2 target. L29, L21, and L26 exhibited the highest values within this range, suggesting enhanced inhibitory activity that correlates with their strong binding affinities and extensive hydrogen bonding interactions. Although L8 and L18 exhibited somewhat lower pIC_{50} values, they still met acceptable criteria for predicted biological activity, supporting their relevance as potential anti-inflammatory agents. These QSAR predictions are indicative and were not derived from a target-specific experimentally validated dataset; therefore, the pIC_{50} values should be interpreted as supportive rather than definitive.

In terms of toxicity predictions, most of the selected molecules exhibited a favorable safety profile compared to the reference drug diclofenac [32]. Each of the compounds was expected

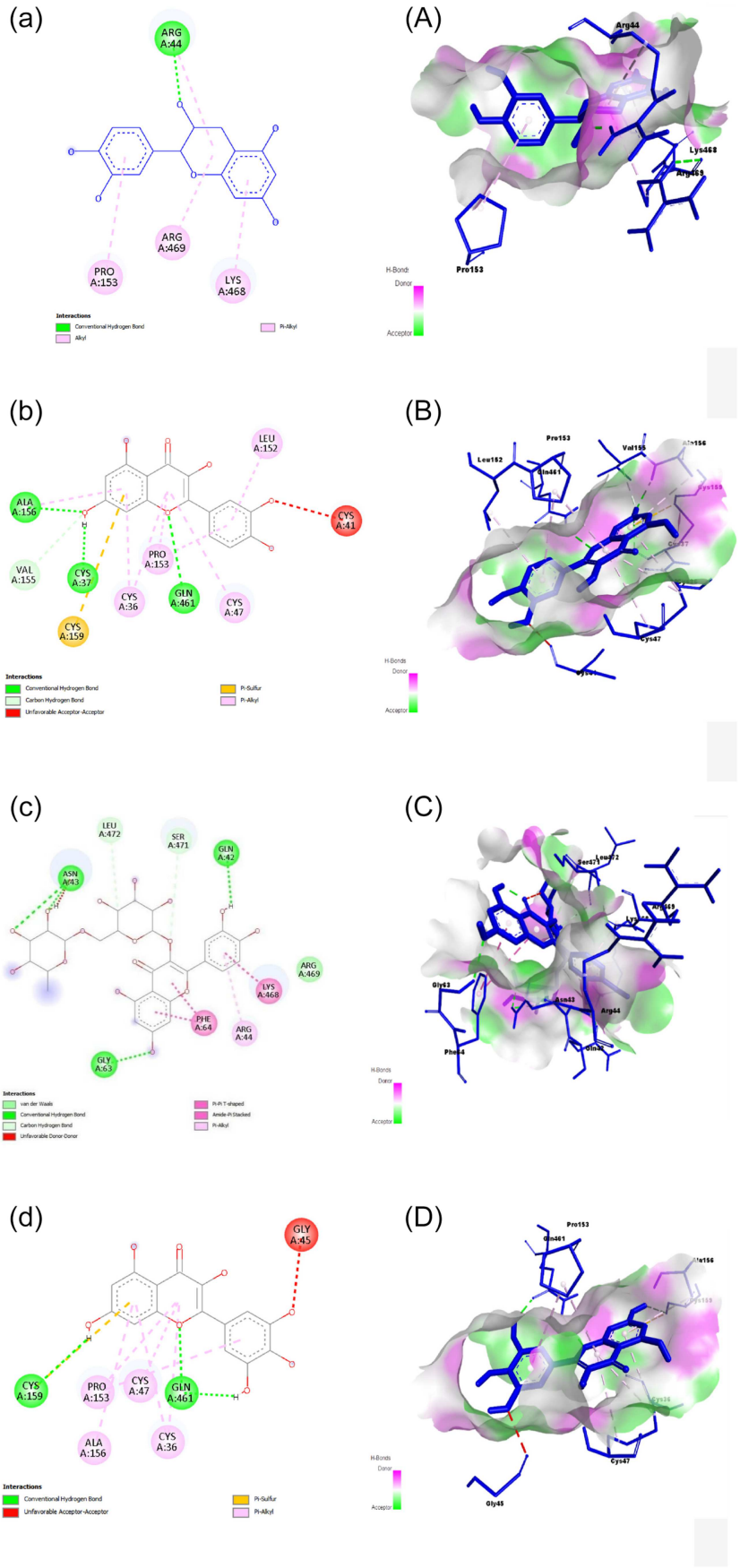
(a)
ARG A:44
ARG A:469
PRO A:153
LYS A:468
Interactions
Conventional Hydrogen Bond
Alkyl
Pi-Alkyl
(A)
Arg44
Lys468
Arg469
Pro153
H-Bonds
Donor
Acceptor
(b)
LEU A:152
ALA A:156
CYS A:41
VAL A:155
CYS A:37
PRO A:153
CYS A:36
GLN A:461
CYS A:47
CYS A:159
Interactions
Conventional Hydrogen Bond
Carbon Hydrogen Bond
Unfavorable Acceptor-Acceptor
Pi-Sulfur
Pi-Alkyl
(B)
Pro153
Leu152
Val155
Gln461
Cys47
H-Bonds
Donor
Acceptor
(c)
LEU A:472
SER A:471
GLN A:42
ASN A:43
ARG A:469
LYS A:468
PHE A:64
ARG A:44
GLY A:63
Interactions
van der Waals
Conventional Hydrogen Bond
Carbon Hydrogen Bond
Unfavorable Donor-Donor
Pi-Pi T-shaped
Amide-Pi Stacked
Pi-Alkyl
(C)
Ser471
Leu472
Arg469
Gly63
Asn43
Arg44
Phe64
H-Bonds
Donor
Acceptor
(d)
GLY A:45
CYS A:159
PRO A:153
CYS A:47
GLN A:461
ALA A:156
CYS A:36
Interactions
Conventional Hydrogen Bond
Unfavorable Acceptor-Acceptor
Pi-Sulfur
Pi-Alkyl
(D)
Pro153
Gln461
Cys47
Gly45
H-Bonds
Donor
Acceptor

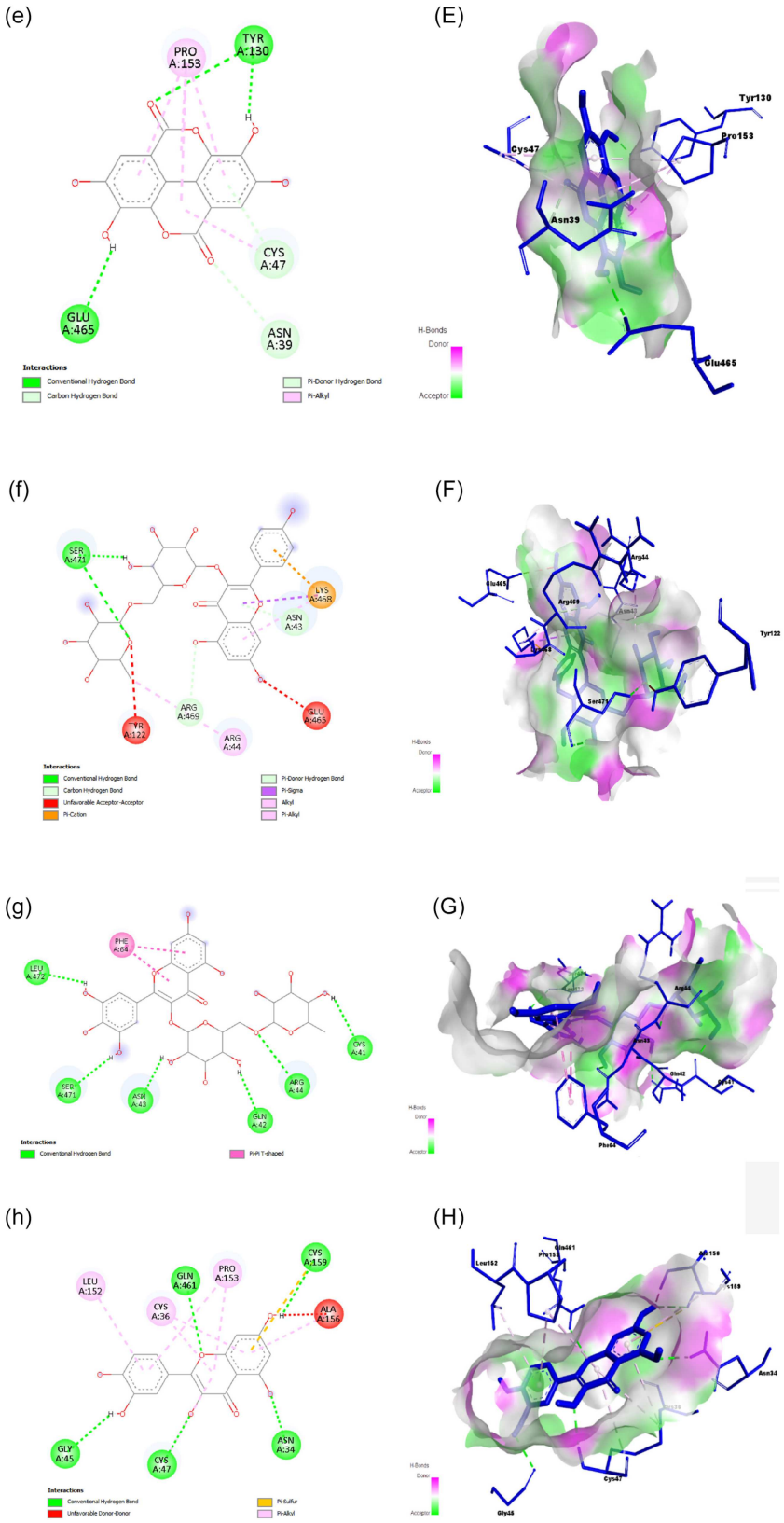

Figure 5. On the left, two-dimensional diagrams of the binding interactions of (a) L8, (b) L18, (c) L21, (d) L24, (e) L25, (f) L26, (g) L29, and (h) L32 with the active site residues of the COX-2 enzyme are shown. Magenta circles indicate polar amino acids, green circles indicate nonpolar amino acids, orange circles indicate positively charged amino acids, red circles represent negatively charged amino acids, and yellow circles denote aromatic residues. On the right, three-dimensional binding poses with hydrogen bonding of (A) L8, (B) L18, (C) L21, (D) L24, (E) L25, (F) L26, (G) L29, and (H) L32 with the active site residues of the COX-2 protein are shown. Ligand atoms are depicted with ball-and-stick models (blue color), and protein residues are represented with stick models

to be inactive in hepatotoxicity and neurotoxicity, which means that it is unlikely to damage the liver and nervous system. However, all ligands showed nephrotoxicity, consistent with the reference drug diclofenac. This might be a potential class-related renal liability that warrants experimental validation. Carcinogenicity was predicted only for a few compounds (L18, L24, L25, and L32), whereas all molecules were found inactive toward cytotoxicity. Nutritional toxicity was inactive or low for most compounds. The predicted LD_{50} values ranged from 159 mg/kg to 10,000 mg/kg, corresponding to toxicity classes 3 to 6 based on the GHS system. Notably, compounds L8 (class VI) and L25, L26, L29 (class V) were categorized as nontoxic or weakly toxic, while the reference drug diclofenac was more toxic (class III). These findings indicate that several of the selected phytochemicals possess comparatively lower toxicity risks than the standard reference drug.

Ecological toxicity assessment likewise revealed favorable profiles for the selected ligands. Predictions suggested low mutagenic, avian, and honey bee toxicity, with substantially lower crustacean, fish, and *T. pyriformis* toxicity compared with diclofenac [51]. Biodegradability scores further emphasized environmental compatibility, particularly for L8, L21, and L29, which demonstrated comparatively higher biodegradability while maintaining low ecotoxicity risk. Overall, the results suggest that these *Amaranthus*-derived compounds, particularly L8, L21, and L29, possess a lower ecological risk and better environmental compatibility, supporting their potential as safer and more sustainable bioactive candidates. The findings from molecular docking, molecular property evaluation, ADMET profiling, QSAR prediction, toxicity assessment, and ecological safety collectively suggest that the selected *A. tricolor* phytochemicals, particularly L29, L24, L18, L32, L8, and L25, demonstrate promising inhibitory potential toward COX-2, along with favorable pharmacokinetic and environmental safety characteristics. These observations, however, are computationally predicted and need experimental validation using compounds.

There are a few limitations in this study. The results are only calculated using computational methods and should be supported by experimental in vitro COX-2 inhibition tests. Direct comparison across docking studies should be interpreted cautiously due to differences in docking engines, scoring functions, and receptor preparation protocols. Future research should focus on *in vitro* testing of the top candidates, including myricetin-3-O-rutinoside, myricetin, and quercetin, to verify their anti-inflammatory potential. This study serves as an exploratory *in silico* screening that relies on static molecular docking. Thus, the results are preliminary and generate hypotheses. To fully validate binding stability, molecular dynamics simulations are also necessary.

5. Conclusion

This study offers a thorough *in silico* assessment of the anti-inflammatory capabilities of phytochemicals derived from *A. tricolor* L. Several plant compounds exhibited a high binding affinity for the COX-2 enzyme, exceeding that of the reference medication diclofenac, and formed stable interactions with critical active-site residues. Among the screened phytochemicals, myricetin-3-O-rutinoside (−10.2 kcal/mol), myricetin (−9.9 kcal/mol), and quercetin (−9.5 kcal/mol), emerged as the most promising COX-2 inhibitors. These candidates warrant immediate validation through molecular dynamics simulations, followed by in vitro COX-2 inhibition assays and in vivo anti-inflammatory studies. Physicochemical and pharmacokinetic evaluations demonstrated that the majority of the top-ranked compounds exhibit satisfactory drug-likeness, moderate bioavailability, and advantageous safety profiles, characterized by limited access to the central nervous system and a minimal risk of cytochrome P450-mediated interactions. QSAR predictions further supported their potential inhibitory activity, while toxicity and ecological assessments suggested comparatively lower toxicity and environmental risk than the standard drug. Overall, the findings demonstrated that phytocompounds from *A. tricolor* can be promising natural COX-2 inhibitors with potential anti-inflammatory activity.

Abbreviations

ADMET:	Absorption, Distribution, Metabolism, Excretion, and Toxicity
BBB:	Blood–Brain Barrier
CNS:	Central Nervous System
COX-2:	Cyclooxygenase-2
CYP450:	Cytochrome P450
GHS:	Globally Harmonized System
HIA:	Human Intestinal Absorption
LD_{50}:	Median Lethal Dose
Log P:	Lipophilicity
Log S:	Aqueous Solubility
NSAID:	Non-Steroidal Anti-Inflammatory Drug
PDB:	Protein Data Bank
QSAR:	Quantitative Structure–Activity Relationship
TPSA:	Topological Polar Surface Area

Acknowledgements

The authors are grateful to the Department of Pharmacy, Bangladesh University, the Department of Pharmacy, East West University, and the Department of Pharmacy, University of Information Technology and Sciences.

Ethical Statement

This work is entirely computational and does not involve human participants or animal experiments. Therefore, ethical approval and informed consent were not required.

Conflicts of Interest

The authors declare that they have no conflicts of interest to this work.

Data Availability Statement

All data generated or analyzed during this study are included in this published article.

Author Contribution Statement

Ferdousi Ahmed Sumona: Software, Investigation, Writing – original draft, Visualization. **Sawda Binta Kamrul Oishi:** Software, Formal analysis, Investigation, Writing – original draft, Visualization. **Md. Rakibul Hossain:** Formal analysis, Investigation, Writing – original draft, Visualization. **Sumaiya Khatun:**

Formal analysis, Investigation, Writing – original draft, Visualization. **Ayesha Islam Sadia:** Formal analysis, Investigation, Writing – original draft, Visualization. **Md. Sabbir Hossain:** Formal analysis, Investigation, Writing – original draft, Visualization. **Md. Abu Bakar Siddique Jami:** Conceptualization, Methodology, Software, Resources, Data curation, Writing – original draft, Writing – review & editing, Visualization, Supervision, Project administration.

References

[1] Calhelha, R. C., Haddad, H., Ribeiro, L., Heleno, S. A., Carocho, M., & Barros, L. (2023). Inflammation: What's there and what's new? *Applied Sciences*, *13*(4), 2312. https://doi.org/10.3390/app13042312

[2] Chavda, V. P., Feehan, J., & Apostolopoulos, V. (2024). Inflammation: The cause of all diseases. *Cells*, *13*(22), 1906. https://doi.org/10.3390/cells13221906

[3] Chen, L., Deng, H., Cui, H., Fang, J., Zuo, Z., Deng, J., . . . , & Zhao, L. (2017). Inflammatory responses and inflammation-associated diseases in organs. *Oncotarget*, *9*(6), 7204–7218. https://doi.org/10.18632/oncotarget.23208

[4] Gaikwad, V. V., Gitaje, S. R., Joshi, S. D., Kharmate, S. V., Phalle, D. R., More, M. P., . . . , & Shingade, P. P. (2025). Mechanisms of inflammation associated with chronic diseases: A brief review. *Journal of Advances in Medicine and Medical Research*, *37*(3), 48–56. https://doi.org/10.9734/jammr/2025/v37i35745

[5] Bhol, N. K., Bhanjadeo, M. M., Singh, A. K., Dash, U. C., Ojha, R. R., Majhi, S., . . . , & Jena, A. B. (2024). The interplay between cytokines, inflammation, and antioxidants: Mechanistic insights and therapeutic potentials of various antioxidants and anti-cytokine compounds. *Biomedicine & Pharmacotherapy*, *178*, 117177. https://doi.org/https://doi.org/10.1016/j.biopha.2024.117177

[6] Hossain, M. S., Jami, M. A. B. S., Ashraful, A. B. M., Uddin, M. N., Sarker, J., Uddin, M. J., . . . , & Alam, A. H. M. (2026). Unveiling the anti-inflammatory activity of chloroform fraction of curcuma wallichii and its phytoconstituents by in vivo and in silico studies. *Scientific Reports*, *16*(1), 1762. https://doi.org/10.1038/s41598-025-28248-3

[7] Ju, Z., Li, M., Xu, J., Howell, D. C., Li, Z., & Chen, F.-E. (2022). Recent development on COX-2 inhibitors as promising anti-inflammatory agents: The past 10 years. *Acta Pharmaceutica Sinica B*, *12*(6), 2790–2807. https://doi.org/10.1016/j.apsb.2022.01.002

[8] Sohail, R., Mathew, M., Patel, K. K., Reddy, S. A., Haider, Z., Naria, M., . . . , & Patel, K. K. (2023). Effects of Non-steroidal Anti-inflammatory Drugs (NSAIDs) and Gastroprotective NSAIDs on the gastrointestinal tract: A narrative review. *Cureus*, *15*(4), e37080. https://doi.org/10.7759/cureus.37080

[9] Deng, W., Du, H., Liu, D., & Ma, Z. (2022). Editorial: The role of natural products in chronic inflammation. *Frontiers in Pharmacology*, *13*, 901538. https://doi.org/10.3389/fphar.2022.901538

[10] Jami, M. A. B. S., Islam, R., Sultana, R., Iffat, T., & Jahan, M. L. (2024). Home remedy practices among stay-at-home COVID-19 patients in Bangladesh. *Medinformatics*, *1*(3), 142–151. https://doi.org/10.47852/bonviewmedin42023132

[11] Roni, M. A. H., Jami, M. A. B. S., Sultana, R., Areefin, P., Hossain, S., Hossain, S., & Hossen, S. (2024). Traditional herbal interventions for premenstrual syndrome management: A comprehensive literature review. *International Journal of Chemical and Biochemical Sciences (IJCBS)*, *25*(18), 120–140.

[12] Debnath, B., Singh, W. S., Das, M., Goswami, S., Singh, M. K., Maiti, D., & Manna, K. (2018). Role of plant alkaloids on human health: A review of biological activities. *Materials Today Chemistry*, *9*, 56–72. https://doi.org/10.1016/j.mtchem.2018.05.001

[13] Gonfa, Y. H., Tessema, F. B., Bachheti, A., Rai, N., Tadesse, M. G., Singab, A. N., . . . , & Bachheti, R. K. (2023). Anti-inflammatory activity of phytochemicals from medicinal plants and their nanoparticles: A review. *Current Research in Biotechnology*, *6*, 100152. https://doi.org/https://doi.org/10.1016/j.crbiot.2023.100152

[14] Sun, W., & Shahrajabian, M. H. (2023). Therapeutic potential of phenolic compounds in medicinal plants-natural health products for human health. *Molecules*, *28*(4), 1845. https://doi.org/10.3390/molecules28041845

[15] Pulipati, S., Babu, P. S., Naveena, U., Parveen, S. K. R., Nausheen, S. K. S., & Sai, M. T. N. (2017). Determination of total phenolic, tannin, flavonoid contents and evaluation of antioxidant property of Amaranthus tricolor (L). *International Journal of Pharmacognosy and Phytochemical Research*, *9*(6), 814–819. https://doi.org/10.25258/phyto.v9i6.8184

[16] Sarker, U., Rabbani, M. G., Oba, S., Eldehna, W. M., Al-Rashood, S. T., Mostafa, N. M., & Eldahshan, O. A. (2022). Phytonutrients, colorant pigments, phytochemicals, and antioxidant potential of orphan leafy amaranthus species. *Molecules*, *27*(9), 2899. https://doi.org/10.3390/molecules27092899

[17] Srivastava, R. (2017). An updated review on phytopharmacological and pharmacognostical profile of Amaranthus tricolor: A herb of nutraceutical potentials. *The Pharma Innovation*, *6*(6), 124–129.

[18] European and Mediterranean Plant Protection Organization (EPPO). (1996). *Amaranthus tricolor (AMATR)*. *EPPO Global Database*. https://gd.eppo.int/taxon/AMATR?utm

[19] Sarker, U., & Oba, S. (2019). Antioxidant constituents of three selected red and green color Amaranthus leafy vegetable. *Scientific Reports*, *9*(1), 18233. https://doi.org/10.1038/s41598-019-52033-8

[20] Al-Dosari, M. S. (2010). The effectiveness of ethanolic extract of Amaranthus tricolor L.: A Natural hepatoprotective agent. *The American Journal of Chinese Medicine*, *38*(06), 1051–1064. https://doi.org/10.1142/S0192415X10008469

[21] Kumar Bs, A. (2025). Amaranthus tricolor: A nutrient-dense functional food with promising therapeutic potential. *International Journal of Pharmaceutical Sciences and Drug Research*, *17*(1), 105–109. https://doi.org/10.25004/IJPSDR.2025.170115

[22] Spórna-Kucab, A., Tekieli, A., Kisiel, A., Grzegorczyk, A., Skalicka-Woźniak, K., Starzak, K., & Wybraniec, S. (2023). Antioxidant and antimicrobial effects of baby leaves of Amaranthus tricolor L. harvested as vegetable in correlation with their phytochemical composition. *Molecules*, *28*(3), 1463. https://doi.org/10.3390/molecules28031463

[23] Singh, M. P., Goel, B., Kumar, R., & Rathor, S. (2024). Phytochemical and pharmacological aspects of genus Amaranthus. *Fitoterapia*, *176*, 106036. https://doi.org/https://doi.org/10.1016/j.fitote.2024.106036

[24] Akhtar, M. A. (2022). Anti-inflammatory medicinal plants of Bangladesh—A pharmacological evaluation. *Frontiers in*

Pharmacology, *13*, 809324. https://doi.org/10.3389/fphar.2022.809324

[25] Jami, M. A. B. S., & Biswas, K. (2023). A cross-sectional study regarding the knowledge, attitude and awareness about self-medication among Bangladeshi people. *Health Policy and Technology*, *14*(4), 100715. https://doi.org/10.1016/j.hlpt.2022.100715

[26] Singh, N., Singh, P., Shevkani, K., & Virdi, A. S. (2019). Amaranth: Potential source for flour enrichment. In *Flour and breads and their fortification in health and disease prevention* (pp. 123–135). Elsevier. https://doi.org/10.1016/B978-0-12-814639-2.00010-1

[27] U.S. Department of Agriculture. (2026). *Classification for Kingdom Plantae Down to Species Amaranthus tricolor L.* USDA Natural Resources Conservation Service. https://plants.usda.gov/classification/55800

[28] Nag, A., Paul, S., Banerjee, R., & Kundu, R. (2021). In silico study of some selective phytochemicals against a hypothetical SARS-CoV-2 spike RBD using molecular docking tools. *Computers in Biology and Medicine*, *137*, 104818. https://doi.org/10.1016/j.compbiomed.2021.104818

[29] Shafiq, N., Mehroze, A., Sarwar, W., Arshad, U., Parveen, S., Rashid, M., . . . , & Bourhia, M. (2023). Exploration of phenolic acid derivatives as inhibitors of SARS-CoV-2 main protease and receptor binding domain: Potential candidates for anti-SARS-CoV-2 therapy. *Frontiers in Chemistry*, *11*, 1251529. https://doi.org/10.3389/fchem.2023.1251529

[30] Singh, A., & Vellapandian, C. (2024). In silico and pharmacokinetic assessment of echinocystic acid effectiveness in Alzheimer's disease like pathology. *Future Science OA*, *10*(1), FSO904. https://doi.org/10.2144/fsoa-2023-0150

[31] De Carlo, A., Ronchi, D., Piastra, M., Tosca, E. M., & Magni, P. (2024). Predicting ADMET properties from molecule SMILE: A bottom-up approach using attention-based graph neural networks. *Pharmaceutics*, *16*(6), 776. https://doi.org/10.3390/pharmaceutics16060776

[32] Banerjee, P., Kemmler, E., Dunkel, M., & Preissner, R. (2024). ProTox 3.0: A webserver for the prediction of toxicity of chemicals. *Nucleic Acids Research*, *52*(W1), W513–W520. https://doi.org/10.1093/nar/gkae303

[33] Siddikey, F., Roni, M. A. H., Kumer, A., Chakma, U., & Matin, M. M. (2022). Computational investigation of Betalain derivatives as natural inhibitor against food borne bacteria. *Current Chemistry Letters*, *11*(3), 309–320. https://doi.org/10.5267/j.ccl.2022.3.003

[34] Gu, Y., Yu, Z., Wang, Y., Chen, L., Lou, C., Yang, C., . . . , & Tang, Y. (2024). admetSAR3.0: A comprehensive platform for exploration, prediction and optimization of chemical ADMET properties. *Nucleic Acids Research*, *52*(W1), W432–W438. https://doi.org/10.1093/nar/gkae298

[35] Kumer, A., Chakma, U., Chandro, A., Howlader, D., Akash, S., Kobir, M. E., . . . , & Matin, M. M. (2022). Modified D-glucofuranose computationally screening for inhibitor of breast cancer and triple breast cancer: Chemical descriptor, molecular docking, molecular dynamics and qsar. *Journal of the Chilean Chemical Society*, *67*(3), 5623–5635. https://doi.org/10.4067/S0717-97072022000305623

[36] Agu, P. C., Afiukwa, C. A., Orji, O. U., Ezeh, E. M., Ofoke, I. H., Ogbu, C. O., . . . , & Aja, P. M. (2023). Molecular docking as a tool for the discovery of molecular targets of nutraceuticals in diseases management. *Scientific Reports*, *13*(1), 13398. https://doi.org/10.1038/s41598-023-40160-2

[37] Imberty, A., Hardman, K. D., Carver, J. P., & Pérez, S. (1991). Molecular modelling of protein-carbohydrate interactions. Docking of monosaccharides in the binding site of concanavalin A. *Glycobiology*, *1*(6), 631–642. https://doi.org/10.1093/glycob/1.6.631

[38] Maheswari, A., & Salamun, D. E. (2023). In silico molecular docking of cyclooxygenase (COX-2), ADME-toxicity and in vitro evaluation of antioxidant and anti-inflammatory activities of marine macro algae. *3 Biotech*, *13*(11), 359. https://doi.org/10.1007/s13205-023-03770-1

[39] Lipinski, C. A. (2004). Lead- and drug-like compounds: The rule-of-five revolution. *Drug Discovery Today: Technologies*, *1*(4), 337–341. https://doi.org/https://doi.org/10.1016/j.ddtec.2004.11.007

[40] Coimbra, J. T. S., Feghali, R., Ribeiro, R. P., Ramos, M. J., & Fernandes, P. A. (2020). The importance of intramolecular hydrogen bonds on the translocation of the small drug piracetam through a lipid bilayer. *RSC Advances*, *11*(2), 899–908. https://doi.org/10.1039/d0ra09995c

[41] Rai, M., Singh, A. V., Paudel, N., Kanase, A., Falletta, E., Kerkar, P., . . . , & Soos, M. (2023). Herbal concoction Unveiled: A computational analysis of phytochemicals' pharmacokinetic and toxicological profiles using novel approach methodologies (NAMs). *Current Research in Toxicology*, *5*, 100118. https://doi.org/https://doi.org/10.1016/j.crtox.2023.100118

[42] Wei, W., Cherukupalli, S., Jing, L., Liu, X., & Zhan, P. (2020). Fsp3: A new parameter for drug-likeness. *Drug Discovery Today*, *25*(10), 1839–1845. https://doi.org/https://doi.org/10.1016/j.drudis.2020.07.017

[43] Prasanna, S., & Doerksen, R. J. (2009). Topological polar surface area: A useful descriptor in 2D-QSAR. *Current Medicinal Chemistry*, *16*(1), 21–41. https://doi.org/10.2174/092986709787002817

[44] Arnott, J. A., & Planey, S. L. (2012). The influence of lipophilicity in drug discovery and design. *Expert Opinion on Drug Discovery*, *7*(10), 863–875. https://doi.org/10.1517/17460441.2012.714363

[45] Delaney, J. S. (2004). ESOL: Estimating aqueous solubility directly from molecular structure. *Journal of Chemical Information and Computer Sciences*, *44*(3), 1000–1005. https://doi.org/10.1021/ci034243x

[46] Yan, A., Wang, Z., & Cai, Z. (2008). Prediction of human intestinal absorption by GA feature selection and support vector machine regression. *International Journal of Molecular Sciences*, *9*(10), 1961–1976. https://doi.org/10.3390/ijms9101961

[47] Geldenhuys, W. J., Mohammad, A. S., Adkins, C. E., & Lockman, P. R. (2015). Molecular determinants of blood-brain barrier permeation. *Therapeutic Delivery*, *6*(8), 961–971. https://doi.org/10.4155/tde.15.32

[48] Zhou, S.-F. (2008). Drugs behave as substrates, inhibitors and inducers of human cytochrome P450 3A4. *Current Drug Metabolism*, *9*(4), 310–322. https://doi.org/10.2174/138920008784220664

[49] Lombardo, F., Obach, R. S., Varma, M. V., Stringer, R., & Berellini, G. (2014). Clearance mechanism assignment and total clearance prediction in human based upon in silico models. *Journal of Medicinal Chemistry*, *57*(10), 4397–4405. https://doi.org/10.1021/jm500436v

[50] Alam, M., Abser, M. N., Kumer, A., Bhuiyan, M. M. H., Akter, P., Hossain, M. E., & Chakma, U. (2023).

Synthesis, characterization, antibacterial activity of thiosemicarbazones derivatives and their computational approaches: Quantum calculation, molecular docking, molecular dynamic, ADMET, QSAR. *Heliyon*, *9*(6), e16222. https://doi.org/10.1016/j.heliyon.2023.e16222

[51] Kawsar, S. M. A., & Kumer, A. (2021). Computational investigation of methyl α-D-glucopyranoside derivatives as inhibitor against bacteria, fungi and COVID-19 (SARS-2). *Journal of the Chilean Chemical Society*, *66*(2), 5206–5214. https://doi.org/10.4067/S0717-97072021000205206

How to Cite: Sumona, F. A., Oishi, S. B. K., Khatun, S., & Sadia, A. I. (2026). Phytochemicals from *Amaranthus tricolor* L. with Potential Anti-Inflammatory Activity: An *In Silico* Molecular Docking, QSAR, and ADMET Study. *Medinformatics*. https://doi.org/10.47852/bonviewMEDIN62028877